Projected trends in high-mortality heatwaves under different scenarios of climate, population, and adaptation in 82 US communities

G. Brooke Anderson[1,✉], **Keith W. Oleson**[2], **Bryan Jones**[3], and **Roger D. Peng**[4]

[1]Department of Environmental & Radiological Health Sciences, Colorado State University, Lake Street, Fort Collins, CO 80521, USA

[2]National Center for Atmospheric Research, Boulder, CO, USA

[3]CUNY Institute for Demographic Research, New York, NY, USA

[4]Johns Hopkins Bloomberg School of Public Health, Baltimore, MD, USA

Abstract

Some rare heatwaves have extreme daily mortality impacts; moderate heatwaves have lower daily impacts but occur much more frequently at present and so account for large aggregated impacts. We applied health-based models to project trends in high-mortality heatwaves, including proportion of all heatwaves expected to be high-mortality, using the definition that a high-mortality heatwave increases mortality risk by 20 %. We projected these trends in 82 US communities in 2061–2080 under two scenarios of climate change (RCP4.5, RCP8.5), two scenarios of population change (SSP3, SSP5), and three scenarios of community adaptation to heat (none, lagged, on-pace) for large- and medium-ensemble versions of the National Center for Atmospheric Research's Community Earth System Model. More high-mortality heatwaves were expected compared to present under all scenarios except on-pace adaptation, and population exposure was expected to increase under all scenarios. At least seven more high-mortality heatwaves were expected in a twenty-year period in the 82 study communities under RCP8.5 than RCP4.5 when assuming no adaptation. However, high-mortality heatwaves were expected to remain <1 % of all heatwaves and heatwave exposure under all scenarios. Projections were most strongly influenced by the adaptation scenario— going from a scenario of on-pace to lagged adaptation or from lagged to no adaptation more than doubled the projected number of and exposure to high-mortality heatwaves. Based on our results, fewer high-mortality heatwaves are expected when following RCP4.5 versus RCP8.5 and under higher levels of adaptation, but high-mortality heatwaves are expected to remain a very small proportion of total heatwave exposure.

✉G. Brooke Anderson, brooke.anderson@colostate.edu.

Introduction

Heatwaves pose risks to human mortality, but the risk associated with any single heatwave depends on many factors, including heatwave length, timing, and intensity. On average, heatwaves increase daily mortality risk by approximately 4 % in the United States (Anderson and Bell 2011), but extreme heatwaves present significantly higher risks—in some cases, more than doubling daily mortality (Vandentorren et al. 2004; Shaposhnikov et al. 2014). High-mortality heatwaves, which we define using a threshold of a 20 % or higher increase in daily mortality risk, have a much higher impact per day than moderate heatwaves, which we define as all other heatwaves. Moderate, but much more common, heatwaves likely account, however, for most heatwave health impacts at present.

Several studies have investigated trends in heatwaves (e.g., Oleson et al. 2015) and extreme heat exposure (e.g., Jones et al. 2015) under various climate change scenarios. These, however, have not distinguished between high-mortality and moderate heatwaves. Other studies have projected the expected number of heatwave-related deaths under future scenarios (e.g., Wu et al. 2014; Mills et al. 2015), but do not provide estimates of how concentrated deaths are likely to be (i.e., are most heatwave-related deaths expected to occur during a few very severe heatwave days, or are they more likely to be spread over many heatwave days?). Existing projections would be complemented by estimates of future trends in high-mortality heatwaves, including what proportion of all heatwaves and heatwave exposure are expected to be from high-mortality heatwaves.

Communities have many choices for how to budget funding to limit heat-related health impacts (Huang et al. 2013). Their decisions could be helped by a better understanding of how heatwave exposure is expected to be distributed in the future between more common, lower risk-per-day events and rare but higher risk-per-day events. Some communities may choose to implement daily interventions during extreme heat, including opening and transporting people to cooling centers and increasing staffing for emergency medical services (Huang et al. 2013; Hondula et al. 2015). These interventions cost a certain amount per day of implementation; these interventions, and even more costly daily interventions, might be reasonable costs during high-mortality heatwaves but unrealistic to implement during most moderate heatwave days. Other interventions aim for heat mitigation (e.g., making land use and building design changes to reduce urban heat island effects) (Huang et al. 2013; Hondula et al. 2015). These interventions could bring more persistent relief during both high-mortality and moderate heatwaves and so may be useful to prioritize if high-mortality heatwaves continue to be very rare.

Further, research on heat mortality projections relies on assumptions that are sensitive to changes in the distribution of heatwave exposure between moderate and high-mortality events. For example, while some projections use a constant effect estimate as the expected increased risk on any heatwave day (e.g., Wu et al. 2014; Stone et al. 2014), effects of a high-mortality heatwave can be much larger than average estimates of mortality risk during a heatwave. If many more heatwaves of the future have characteristics that drive them towards effects in the skewed right tail of the distribution of heatwave effects, it would mean that (1) the average heatwave relative risks based on current samples of heatwaves could be much

too low; and (2) uncertainty analysis for heatwave impacts (e.g., Wu et al. 2014) could be too conservative. Further, short-term mortality displacement patterns have been found to vary with heatwave strength (Saha et al. 2014), and some high-mortality heatwaves have been characterized by mid-term mortality displacement, with lower-than-expected mortality rates during approximately a year following the event (Shaposhnikov et al. 2015; Toulemon and Barbieri 2008).

Here, we project trends in high-mortality heatwaves. We project these trends, including estimates of how heatwave exposure is expected to be distributed between high-mortality and moderate heatwaves, in 82 US communities under different scenarios for 2061–2080 of climate change, population growth, and adaptation to changing temperatures. To make these projections, we use health-based classification models developed and tested in a companion paper (Anderson et al., submitted). The models input all heatwaves identified for a certain scenario (using the definition that a heatwave is a period of two or more days above the community's 98th percentile temperature) and then predict which of those are likely high-mortality and which are likely moderate.

We developed the models using, as potential predictive variables, 20 different heatwave characteristics (Table 1), including absolute and relative (compared to the community's typical temperatures) temperature, length (both total length and measures of how many days in the heat wave exceeded a certain absolute or relative temperature), timing, and properties of the community in which the heat wave occurred (population, climate). Previous research has found that these characteristics might affect heat-related danger (Anderson and Bell 2011; Curriero et al. 2002). The heatwave characteristics that each model ultimately incorporated are shown in Table 1.

We trained the models using 19 years of health and weather data from 82 US communities. We fit several different classification trees or ensembles of classification trees. This model structure is useful in describing relationships that are strongly interactive—for example, if a heat wave will only be high-mortality if it is both very intense and occurs early in the summer. We used Monte Carlo cross-validation to assess performance of these models (Kuhn and Johnson 2013) and selected four health-based classification models to use in the current study.

This study is part of a larger project on the Benefits of Reducing Anthropogenic Climate changE (BRACE; O'Neill and Gettelman, submitted). BRACE focuses on characterizing the difference in impacts driven by climate outcomes resulting from the forcing associated with RCP8.5 and RCP4.5 (van Vuuren et al. 2011).

2 Materials and methods

Within 82 US study communities, we projected, for 2061–2080, both the number of and person-days of exposure to high-mortality heatwaves, as well as the percent of heatwaves and heatwave exposure expected to be from high-mortality heatwaves. We projected these trends for twelve scenario combinations: every combination of (1) two scenarios of climate change; (2) two scenarios of population change; and (3) three scenarios of adaptation to

heat. This resulted in 258 different projections once all ensemble members for each of the two climate scenarios were considered. Our analysis covered the 82 US communities used previously to develop our health-based models (Fig. 1; Anderson et al., submitted). Each community is a county or collection of contiguous counties, and all have populations of 300,000, based on the 2000 US Census.

We considered two scenarios of future greenhouse gas forcings, RCP4.5 and RCP8.5 (van Vuuren et al. 2011). In RCP4.5, radiative forcing stabilizes at 4.5 W/m^2 by 2100 without overshoot, representing a scenario in which policy reduces greenhouse gas emissions (Thomson et al. 2011). In RCP8.5, radiative forcing rises to 8.5 W/m^2 by 2100 and continues rising, describing the most extreme greenhouse gas emission pathway of the four RCPs (Riahi et al. 2011).

In modeling projections by climate scenario, we explored how internal climate variability introduced uncertainty into projections. Weather in a location fluctuates around the location's long-term climate. While these random fluctuations have little impact on large-scale, averaged projections (e.g., mean yearly global temperature), they can introduce substantial uncertainty into projections of extremes or trends at the local or regional scale (Hawkins and Sutton 2009; Deser et al. 2014). We explored these uncertainties in our projections by using large- and medium-ensemble models, in which many ensemble members are generated from the same climate model, but with very small changes in the initial conditions.

We use the National Center for Atmospheric Research's (NCAR's) Community Earth System Model (CESM) large ensemble (CESM-LE) as projections of future weather conditions under the Representative Concentration Pathway 8.5 (RCP8.5) scenario of climate change (Kay et al. 2014) and the medium ensemble (CESM-ME) as projections of future weather conditions under Representative Concentration Pathway 4.5 (RCP4.5) (Sanderson et al. 2015). These simulations replay the 20–21st century (1920–2100) 30 times under historical and RCP8.5 external forcing with small atmospheric initial condition differences (Kay et al. 2014).

The model includes a land surface model with an urban component that captures the urban heat island effect, which we used to better represent urban temperature for our projections, rather than using a grid-averaged value averaged over all land surface types (Oleson et al. 2015). Because urban data were not available for the first ensemble member of each scenario, we used 29 ensemble members for RCP8.5 and 14 for RCP4.5. This model's urban heat island estimates are consistent with remote-sensing results (Zhao et al. 2014).

Climate models have been found to have difficulties in projecting of temperature extremes (e.g., temperatures above a certain percentile; Keellings 2016). The climate model used in our study, however, has been found to perform fairly well in projecting extremes (Sillman et al. 2013). Further, calibration can help reduce bias in projecting temperature extremes (Bellprat and Doblas-Reyes 2016); all temperature projections used in this study were bias-corrected using quantile remapping (Online Resource of Oleson et al. 2015).

Within all simulations, we identified all heatwaves based on a definition of a heatwave as ≥ 2 days with T_{mean} > 98th percentile of community's year-round T_{mean} in the present day (1981–2005) (Oleson et al. 2015). This step of the analysis identified all heatwaves within a projection; the health-based models used this set of heatwaves as candidates for high-mortality heatwaves. For each heatwave, we measured all characteristics in Table 1. Descriptions of regional- and community-scale patterns of climate-related heatwave characteristics (e.g., intensity, length) are provided in Oleson et al. (2015). Some heatwave characteristics depended on scenarios of population. To generate population estimates for the study communities for 2061–2080, we used a gravity-type downscaling model (Jones and O'Neill 2013) to create gridded projections of the US population for two Shared Socioeconomic Pathways (SSP3 and SSP5). We then aggregated grid-cell population up to the county-level for each study community (Fig. 1; O'Neill et al. 2015; Jones et al. 2015).

These SSPs provide scenarios of alternative futures in terms of demographic and socioeconomic structure from which we can derive projections of future population (Samir and Lutz 2014). For the US, the SSP3 pathway is characterized by low fertility rates and low rates of in-migration, which leads to an aging population that declines in size over time. The SSP5 pathway is characterized by above-replacement fertility and higher rates of in-migration for the US, leading to a significantly larger population. The downscaling procedure allows for consideration of local patterns of spatial population change (e.g., urban sprawl or consolidation) implicit in the SSP narratives. The fossil-fuel based development specified by SSP5 implies a more sprawling pattern of development than in the more fragmented world implied by SSP3.

These population projections are subject to several sources of uncertainty, including the underlying assumptions regarding fertility, mortality, and migration used to construct the national-level projections for each scenario and the assumptions regarding spatial patterns of development implicit in the downscaling procedure. However, these projections are also internally consistent with the broader SSP narratives and represent a possible outcome given the assumptions associated with each scenario.

We also explored how different assumptions about adaptation influenced projections. If a community adapts to more frequent extreme heat, the same temperature that is currently dangerous in a community might not be as dangerous in the future (Kinney et al. 2008; Huang et al. 2011). Current epidemiological research suggests adaptation to heat, with higher absolute temperatures required to elicit a health response in hot climates compared to milder ones (e.g., Curriero et al. 2002) and in hotter areas of a city compared to cooler areas (Milojevic et al. 2016). We used temperature distributions from different time periods between the present and the future projection period as baselines when calculating relative metrics of temperature during each heatwave (i.e., how hot a heatwave was compared to the climate of a community), which were included in our health-based classification models (Table 1).

We considered three assumptions of how communities might adapt to increasing extreme heat exposure: no adaptation, lagged adaptation, and on-pace adaptation. The "no adaptation" scenario assumes communities will remain adapted to their present-day climate

and not adjust to the higher temperatures more common in the future. For this scenario, we used recent (1981–2005) community temperature distributions to calculate relative heatwave characteristics for future heatwaves. The "lagged adaptation" scenario assumes communities will adapt to, but not keep pace with, climate change. For this, we used community temperature distributions for 2023–2042, a period midway between the future projection period and the present, as a baseline when calculating relative metrics. Finally, for "on-pace adaptation", which assumed communities keep pace with climate change and will be fully adapted to their 2061–2080 climate, we used community temperature distributions from 2061 to 2080 to calculate relative heatwave characteristics.

Once we identified and characterized all heatwaves in a simulation, we used the health-based models developed in Anderson et al. (submitted) to predict which of these heatwaves were expected to be high-mortality versus moderate. We provide full details on the building, evaluation, and selection of these models in our companion paper (Anderson et al., submitted), and the models and a short tutorial on their use are available on GitHub (https://github.com/geanders/HyperHeatwavePredictiveModels).

The classification models, when applied to all heatwaves in a simulation, output two values: H_{ph}, number of heatwaves for the ensemble member predicted by the model to be high-mortality heatwaves, and H_{pm}, number of heatwaves predicted to be moderate. Because the models all had low positive predictive values (~3 %; Anderson et al., submitted), and so resulted in many false positives in their initial classifications, we adjusted initial projections of the total number of high-mortality heatwaves using estimates of the models' performance from Monte Carlo cross-validation (Anderson et al. submitted). These models were estimated to have false omission rates of 0 %, making adjustment for false negatives unnecessary. To estimate the number of high-mortality heatwaves, H_h, we used:

$$H_h = H_{ph} * P$$

where P is estimated model positive predictive value.

To estimate exposure to high-mortality heatwaves, E_h, we summed the product of the lengths and community populations associated with, separately, high-mortality and moderate heatwaves, and then adjusted estimates based on the positive predictive value for the healthbased model:

$$E_h = P \sum_i (D_i N_i)$$

where P is model positive predictive value, i is a heatwave classified as a high-mortality heatwave, with the summation summing over all heatwaves in this classification, D_i is the length of heatwave i in days, and N_i is the population of the community in which heatwave i occurred.

To provide a comparison to present-day trends, we also estimated the number of and exposure to high-mortality heatwaves with ensemble-member data from a 25-year current

period (1981–2005). Since this baseline period is longer (25 years) than the future scenario periods (20 years), we re-scaled the present-day projections to the expected number per 20 years. Since we generated exposure projections in units of millions of person-days per year, the exposure measure did not require re-scaling.

To investigate how projections were influenced by the choice between health-based models, we repeated the process using four different health-based models. We considered a classification tree model, a bagging model, and a boosting model. These different models include different heatwave characteristics as predictors (Table 1), with the bagging model incorporating many heatwave characteristics (although some with low variable importance [Anderson et al. submitted] and so with a small impact on final projections), the boosting model incorporating fewer characteristics, and the classification tree based on only two characteristics (a metric of relative temperature and the month in which the heatwave started).

Because of the rarity of high-mortality heatwaves in the training dataset and the multi-level grouping of heatwaves by regional weather systems, we were somewhat concerned that these three health-based classification models may have overfit to characteristics that are constant or nearly constant across all heatwaves in a regional weather system, like the month in which the heatwave started. Therefore, we also created a customized, simplified model that included only the predictor assessed as being most useful in classifying high-mortality heatwaves—the relative intensity of the highest mean temperature during the heatwave compared to the temperature distribution in the heatwave's community (see Anderson et al., submitted). To test sensitivity to our choice of threshold for high-mortality heatwaves, we also created projections using health-based models that were developed using a slightly lower threshold: 19 % or higher increase in mortality risk (we also considered a slightly higher threshold of 21 % but obtained identical health-based models as the main models using the 20 % threshold).

Results

High-mortality heatwaves were expected to be much more common than at present under all scenarios except those assuming on-pace adaptation (Table 2, top; Fig. 2a). Community-specific results for this and other findings are provided and discussed in the Online Resource. Under all scenarios considered, high-mortality heatwaves were expected to represent less than 1 % of all heatwaves identified with the study's definition (two or more days above the community's present 98th percentile temperature).

When comparing the two climate scenarios, high-mortality heatwaves were generally less frequent under RCP4.5 than RCP8.5, suggesting some high-mortality heatwaves would be avoided under RCP4.5 compared to RCP8.5 (results were almost identical when analysis for RCP8.5 was restricted to the same 14 ensemble members used for RCP4.5; Online Resource Table S1). The difference between the two climate scenarios depended strongly on assumptions about adaptation. Projections differed most between the climate scenarios under the "No Adaptation" scenario: at least 7 additional high-mortality heatwaves were projected over the 82 study communities for the 20-year period for RCP8.5 compared to RCP4.5,

depending on ensemble member and health model (Table 2, top). By comparison, approximately 6 high-mortality heatwaves were projected for the present day, so this difference represents an increase between the two scenarios of more than the total number of high-mortality heatwaves currently expected. The projected number of high-mortality heatwaves differed less between the two climate projections for the "lagged adaptation" scenario, and slightly reversed (i.e., more under RCP4.5 than RCP8.5) for "on-pace adaptation" (Table 2, top; Fig. 2a).

Exposure to high-mortality heatwaves increased substantially compared to the present day across all scenarios considered, although the exact increase differed by scenario (Table 2, bottom; Fig. 2b). Exposure to high-mortality heatwaves was projected to be a very small percentage of total heatwave exposure under all scenarios (Table 2, bottom). Heatwaves tended to be longer under the RCP8.5 scenario (Oleson et al. 2015); therefore, although there were not always large increases in the frequency of high-mortality heatwaves under the RCP8.5 scenario compared to the RCP4.5 scenario (Table 2, top), the scenarios differed in the projected person-days of exposure to high-mortality heatwaves, with a > 70 % increase in exposure for RCP8.5 versus RCP4.5 under a scenario of no adaptation and more than a doubling in exposure for RCP8.5 versus RCP4.5 under a scenario of lagged adaptation (Table 2, bottom).

Population and population density did not influence the projected number of high-mortality heatwaves (Table 2, top). Population growth scenarios did, however, alter projections of person-days of exposure (Table 2, bottom; Fig. 2b) since more people would be exposed to a high-mortality heatwave in a higher-population city. Projected exposure increased by 60–90 % for the SSP5 population scenario compared to SSP3, depending on adaptation and climate scenarios.

The choice of adaptation assumption created the largest variations in projections of both the number of and exposure to high-mortality heatwaves. The projected number of high-mortality heatwaves more than halved when moving from a scenario of no adaptation to lagged adaptation or from lagged to on-pace adaptation (Table 2, top; Fig. 2a). The adaptation scenario also drove trends in exposure projections, with typically more than a halving in projected exposure when moving from the no to lagged adaptation scenario or from the lagged to on-pace adaptation scenario (Table 2, bottom; Fig. 2b).

When comparing across health-based models, we found that projections of the number of and exposure to high-mortality heatwaves varied across the four models (classification tree, bagging, boosting, and custom simplified models) (Table 2). For example, we found the ensemble mean for the projected number of heatwaves for one scenario combination (climate scenario: RCP8.5; adaptation scenario: no adaptation; population scenario: SSP5) ranged from 43 to 76 across the four health-based models. Although projections were not identical, all four health-based models resulted in similar trends when comparing across different scenarios of adaptation, climate change, and population growth. For example, the adaptation scenario was consistently the strongest driver of trends in projections, and high-mortality heatwaves were usually expected to be more common under climate change than at present. We also tested sensitivity of the results to the threshold for defining high-mortality

heatwaves, one of the parameters used when developing the health-based models (Anderson et al., submitted). We found again that exact projections were variable but that general conclusions were consistent—projected frequencies and exposures were most strongly influenced by assumptions about adaptation, and exposure to high-mortality heatwaves was always expected to increase compared to present.

We explored the uncertainty based on internal climate variability by investigating differences in projections across different ensemble members for each scenario (Fig. 2). Trends in heatwave frequency were consistent across ensemble members when comparing adaptation scenarios. While all ensembles projected more high-mortality heatwaves under future scenarios than at present from every scenario except full adaptation, trends in frequency showed some overlap between RCP4.5 and RCP8.5 projections (Fig. 2a). Exposure projections showed similar patterns for uncertainty related to internal climate variability, although these projections were somewhat less sensitive to ensemble variations when comparing results for RCP8.5 versus RCP4.5 (Fig. 2b).

Discussion

Here, we projected how often high-mortality heatwaves are likely to occur under various future scenarios of climate change, population change, and adaption. We found sources of uncertainty in these projections, including from internal climate variability and choice of health-based model. However, we consistently found: (1) an increase compared to present in the number of high-mortality heatwaves under all scenarios except on-pace adaptation; (2) an increase in exposure to high-mortality heatwaves compared to present under all scenarios; and (3) that high-mortality heatwaves were expected, under all scenarios, to comprise less than 1 % of all heatwaves and all heatwave exposures for heatwaves identified using the current definition (two or more days at or above the 98th percentile of the community's current temperatures). Although in some cases more high-mortality heatwaves were projected under the RCP4.5 than RCP8.5 scenario, this finding could result from heatwaves being longer under RCP8.5 (Oleson et al. 2015), which could, in some cases, result in a single long heatwave rather than multiple shorter heatwaves. This hypothesis is supported by our finding that person-days of exposure to high-mortality heatwaves is always projected to be higher under RCP8.5 than RCP4.5.

Based on our findings, although high-mortality heatwaves are expected to occur more frequently in the future under most scenarios considered than at present, they are expected to continue to be a very small fraction of all heatwaves and all heatwave exposure. This finding suggests that interventions planned for only very severe heatwaves could miss most of the exposures that result in heatwave-related mortality. Further, our results suggest that there is unlikely to be a large shift in the proportion of high-mortality heatwaves among all heatwaves, and so potential biases in health impact assessments that could be caused by such a shift are unlikely, and resulting uncertainty in mortality projections is likely small compared to uncertainty introduced from other assumptions required when making heat mortality projections.

In developing the models used here, we found that all high-mortality heatwaves in the training data shared the meteorological characteristic of having at least 1 day at or above the community's 99.89th percentile temperature (Anderson et al., submitted). Because this relative temperature characteristic was very important in all of the health-based classification models, projected trends in high-mortality heatwaves varied most strongly across scenarios of adaptation (Fig. 2, Table 2). Given how strongly adaptation assumptions influenced our projections, future research on the health impacts of heat exposure from climate change should address adaptation assumptions.

Many previous projections of heat-related mortality have been limited to a scenario of "no adaptation" (e.g., Kingsley et al. 2016; Wu et al. 2014). Based on epidemiological studies of the current relationship between heat and health, there is evidence that this scenario is less likely than a scenario of at least some adaptation, both intentional (e.g., urban planning, community-directed heat warning systems) and unintentional (e.g., acclimatization, improvements in population health) (Hondula et al. 2015). For example, one study explored the relationship between heat and health within parts of London with differing temperatures, because of differing heat island effects, and found that evidence was inconsistent with a "no acclimatization" assumption (Milojevic et al. 2016).

A few projections have explored adaptation scenarios using different approaches (Hondula et al. 2015). Some studies have used adaptation scenarios where temperature-mortality models were developed using only the hottest recent summers (e.g., Hayhoe et al. 2004). These scenarios would likely incorporate only short-term adaptation (e.g., acclimatization, immediate behavior changes), not longer-term adaptation (e.g., changes in building or urban design). Other projections have assumed all communities will adapt by a certain absolute increase in temperature (e.g., temperature-mortality curves will shift right along the temperature axis) (Gosling et al. 2009). While these scenarios are similar to our scenario of "lagged" adaptation, in allowing some adaptation to heat, they assume that all communities will adapt to the same absolute increase in temperature, while our scenarios assume that communities with greater changes in temperature distributions will also have greater changes in adaptation. Other projections have used created temperature-mortality curves in "analog" cities that currently have the anticipated future climate of the city for which projections are being done (e.g., Knowlton et al. 2007; Mills et al. 2015). This analog city approach is conceptually similar to our scenario of on-pace adaptation. However, if community characteristics like urban design and demographics are likely to be more similar between a city at present and the same city during the future projection period than between the future city and its analog city at present, however, then our approach may provide a better representation of a scenario of full adaptation.

While scenarios of "no adaptation" and "full adaptation" represent a wide range of adaptation scenarios, these are not the outer limits of possible adaptation scenarios. Feasibly, communities could do worse than "no adaptation"—for example, if power grids deteriorate, a community may respond worse in the future than it currently does to similar temperatures. Alternatively, technological and health advances may allow communities to handle temperature distributions of the future even better than they handle today's climate, leading to better adaptation than that portrayed by the "on-pace adaptation" scenario. There is

evidence of decreasing susceptibility to heat in the US over the past decades (Gasparrini et al. 2015; Bobb et al. 2014), which suggests that this scenario of more adaptation than in our "on-pace" scenario would also be realistic to consider. To explore adaptation assumptions in future health impacts research, it may be useful to expand the approach we used here and use temperature-mortality curves fit to relative, rather than absolute, temperature (e.g., the curves developed in Gasparrini et al. 2015), as well as incorporate estimates of the declining trend in heat susceptibility in the US found by Bobb et al. (2014) and Gasparrini et al. (2015).

Our adaptation scenarios were not based on specific practices of adaptation that communities are expected to take; rather, they span a range of possible scenarios of adaptation. This simplified approach allowed a preliminary investigation of the role that adaptation assumptions make in introducing uncertainty in projected trends in high-mortality heatwaves. While it would be preferable to model adaptation based on scenarios of specific adaptation measures, there are not clear estimates of the effect modification expected from different adaptation strategies (Boeckmann and Rohn 2014), and some of the trends in adaptation might result from decreasing susceptibility to heat unrelated to planned adaptations.

Our study explored uncertainty in projections related to the choice of health-based model and to internal climate variability. There are other sources of uncertainty in projections, however, that this study did not capture. For example, while we used a large-ensemble model to try to characterize uncertainty introduced by internal climate variability, some climate model uncertainty persists beyond that captured by comparing projections across ensemble members. We have not, for example, explored climate model structural uncertainty or uncertainty in climate model parameters (e.g., climate sensitivity) (Monier et al. 2014), which can introduce uncertainty in health impact estimates (e.g., Kingsley et al. 2016; Gosling et al. 2012). We were unable to explore these sources of uncertainty since, to our knowledge, only one other model submitted to CMIP5 provides urban output (McCarthy et al. 2010), and it uses a different urban representation than the model used here.

Further, while the climate model we used provides urban climate output, this urban representation does not capture fine-scale or temporal variations in urban form within study communities. In our urban modeling, there are only six unique sets of urban properties over the US, which means that some communities share the same morphological, thermal, and radiative characteristics in the model, and there is no variation in climate projections within a community (Oleson et al. 2015). Some studies have found heat-health effects can vary at finer scales, including within cities, based on differences in urban form (Burkart et al. 2016; Jenerette et al. 2016) and that warming projections can be strongly influenced by within-community scenarios of urban expansion (Georgescu et al. 2014). This level of within-community variation would not be captured by the projections we used. Our climate model also assumes urban areas are static in time, and it does not incorporate population effects on future urban extent and properties. If it did, the population scenario might have influenced temperature projections and so influenced more of the model characteristics than those identified as population-related in Table 1. It may be possible to explore this dynamic more

in the future, as climate models develop to be able to incorporate scenarios of changing urban form.

Results presented here rely on certain health modeling choices, including the heatwave definition used to identify all heatwaves in future temperature projections. We identified the set of all heatwaves in a projection using, as a threshold, a community's 98th percentile of present-day temperatures. Temperatures that are currently extreme are likely to be much more common toward the end of the 21st century (Diffenbaugh et al. 2011), and heat mortality projections that estimate an average effect for all heatwave days have been found to be sensitive to the heatwave definition used (Wu et al. 2014). Our estimates of the frequency of and exposure to high-mortality heatwaves are not likely to be sensitive to the heatwave definition in the same way, as our estimates use models that count only heatwaves with characteristics that make them more likely to be high-mortality. However, our estimates of the proportion of all heatwaves or heatwave exposure that are expected to be high-mortality could be more sensitive to this heatwave definition, since these estimates use, as a denominator, the total number of heatwaves or heatwave exposure identified in a projection.

While our health-based model building found that most high-mortality heatwaves share certain meteorological characteristics, particularly a very high relative temperature, many moderate heatwaves also have these characteristics, which resulted in the health-based models having low positive predictive values (Anderson et al. submitted). While we adjusted for this in our projections using estimates of model performance from Monte Carlo cross-validation (Anderson et al. submitted), it would be preferable for future research to develop models with better positive predictive values. The health impacts of heat vary by personal susceptibility factors like age (Anderson and Bell 2009), and heat effects might be compounded by concurrent exposures like high air pollution or power outages. Future research could explore whether additional characteristics could improve classification models for heatwaves, as well as whether such characteristics could be projected for future heatwaves with enough resolution to be usefully incorporated into projections.

Supplementary Material

Refer to Web version on PubMed Central for supplementary material.

Acknowledgments

References

Anderson GB, Bell ML. Weather-related mortality: how heat, cold, and heat waves affect mortality in the United States. Epidemiology. 2009; 20(2):205–213. [PubMed: 19194300]

Anderson GB, Bell ML. Heat waves in the United States: mortality risk during heat waves and effect modification by heat wave characteristics in 43 US communities. Environ Health Perspect. 2011; 119(2):210–218. [PubMed: 21084239]

Bellprat O, Doblas-Reyes F. Attribution of extreme weather and climate events overestimated by unreliable climate simulations. Geophys Res Lett. 2016; 43:2158–2164.

Bobb JF, Peng RD, Bell ML, Dominici F. Heat-related mortality and adaptation to heat in the United States. Environ Health Perspect. 2014; 122(8):811–816. [PubMed: 24780880]

Boeckmann M, Rohn I. Is planned adaptation to heat reducing heat-related mortality and illness? A systematic review. BMC Public Health. 2014; 14:1112. [PubMed: 25349109]

Burkart K, Meier F, Schneider A, et al. Modification of heat-related mortality in an elderly urban population by vegetation (urban green) and proximity to water (urban blue): evidence from Lisbon, Portugal. Environ Health Perspect. 2016

Curriero F, Heiner K, Samet J, et al. Temperature and mortality in 11 cities of the eastern United States. Am J Epidemiol. 2002; 155(1):80–87. [PubMed: 11772788]

Deser C, Phillips AS, Bourdette V, Teng H. Projecting north American climate over the next 50 years: uncertainty due to internal variability. J Clim. 2014; 27:2271–2296.

Diffenbaugh NS, Ashfaq M, Scherer M. Transient regional climate change: analysis of the summer climate response in a high-resolution, century-scale ensemble experiment over the continental United States. J Geophys Res. 2011; 116:D24111.

Gasparrini A, Guo Y, Hashizume M, et al. Temporal variation in heat-mortality associations: a multicountry study. Environ Health Perspect. 2015; 123:1200–1207. [PubMed: 25933359]

Georgescu M, Morefield PE, Bierwagen BG, Weaver CP. Urban adaptation can roll back warming of emerging megapolitan regions. Proc Natl Acad Sci. 2014; 111(8):2909–2914. [PubMed: 24516126]

Gosling SN, McGregor GR, Lowe JA. Climate change and heat-related mortality in six cities. Part 2: climate model evaluation and projected impacts from changes in the mean and variability of temperature with climate change. Int J Biometeorol. 2009; 53(1):31–51. [PubMed: 19052780]

Gosling SN, McGregor GR, Lowe JA. The benefits of quantifying climate model uncertainty in climate change impacts assessment: an example with heat-related mortality change estimates. Clim Chang. 2012; 112:217–231.

Hawkins E, Sutton R. The potential to narrow uncertainty in regional climate predictions. Bull Am Meteorol Soc. 2009; 90:1095–1107.

Hayhoe K, Cayan D, Field CB, et al. Emissions pathways, climate change, and impacts on California. Proc Natl Acad Sci. 2004; 101(34):12422–12427. [PubMed: 15314227]

Hondula DM, Balling RC, Vanos JK, Georgescu M. Rising temperatures, human health, and the role of adaptation. Curr Clim Chang Rep. 2015; 1(3):144–154.

Huang C, Barnett AG, Wang X, et al. Projecting future heat-related mortality under climate change scenarios: a systematic review. Environ Health Perspect. 2011; 119(12):1681–1690. [PubMed: 21816703]

Huang C, Barnett AG, Xu Z, et al. Managing the health effects of temperature in response to climate change: challenges ahead. Environ Health Perspect. 2013; 121(4):415–419. [PubMed: 23407064]

Jenerette GD, Harlan SL, Buyantuev A, et al. Micro-scale urban surface temperatures are related to land-cover features and residential heat related health impacts in Phoenix, AZ USA. Landsc Ecol. 2016; 31:745–760.

Jones B, O'Neill B. Historically grounded spatial population projections for the continental United States. Environ Res Lett. 2013; 8(4):044021.

Jones B, BC O'N, McDaniel L, McGinnis S, Mearns LO, Tebaldi C. Future population exposure to US heat extremes. Nat Clim Chang. 2015; 5(7):652–655.

Kay JE, Deser C, Phillips A, et al. The Community Earth System Model (CESM) large ensemble project: a community resource for studying climate change in the presence of internal climate variability. Bull Am Meteorol Soc. 2014

Keellings D. Evaluation of downscaled CMIP5 model skill in simulating daily maximum temperature over the southeastern United States. Int J Climatol. 2016

Kingsley SL, Eliot MN, Gold J, Vanderslice RR, Wellenius GA. Current and projected heat-related morbidity and mortality in Rhode Island. Environ Health Perspect. 2016

Kinney PL, O'Neill MS, Bell ML, Schwartz J. Approaches for estimating effects of climate change on heat-related deaths: challenges and opportunities. Environ Sci Pol. 2008; 11(1):87–96.

Knowlton K, Lynn B, Goldberg RA, et al. Projecting heat-related mortality impacts under a changing climate in the New York City region. Am J Public Health. 2007; 97:2028–2034. [PubMed: 17901433]

Kuhn, M., Johnson, K. New York: Springer; 2013. Applied predictive modeling.

McCarthy MP, Best MJ, Betts RA. Climate change in cities due to global warming and urban effects. Geophys Res Lett. 2010; 37:L09705.

Mills D, Schwartz J, Lee M, Sarofim M, Jones R, Lawson M, Duckworth M, Deck L. Climate change impacts on extreme temperature mortality in select metropolitan areas in the United States. Climatic Change. 2015; 131(1):83–95.

Milojevic A, Armstrong BG, Gasparrini A, Bohnenstengel SI, Barratt B, Wilkinson P. Methods to estimate acclimatization to the Urban Heat Island effects on heat- and cold-related mortality. Environ Health Perspect. 2016

Monier E, Gao X, Scott JR, et al. A framework for modeling uncertainty in regional climate change. Clim Change. 2014

O'Neill BC, Kriegler E, Ebi KL, et al. The roads ahead: Narratives for shared socioeconomic pathways describing world futures in the 21st century. Glob Environ Chang. 2015

Oleson KW, Anderson GB, Jones B, et al. Avoided climate impacts of urban and rural heat and cold waves over the U.S using large climate model ensembles for RCP8.5 and RCP4.5. Clim Chang. 2015

Riahi K, Rao S, Krey V, et al. RCP 8.5—a scenario of comparatively high greenhouse gas emissions. Clim Chang. 2011; 109:33–57.

Saha MV, Davis RE, Hondula DM. Mortality displacement as a function of heat event strength in 7 US cities. Am J Epidemiol. 2014; 179(4):467–474. [PubMed: 24264293]

Samir KC, Lutz W. The human core of the shared socioeconomic pathways: population scenarios by age, sex and level of education for all countries to-2100. Glob Environ Chang. 2014

Sanderson BM, Oleson KW, Strand WG, O'Neill BC. A new ensemble of GCM simulations to assess avoided impacts in a climate mitigation scenario. Clim Chang. 2015 in review.

Shaposhnikov D, Revich B, Bellander T, et al. Mortality related to air pollution with the Moscow heat wave and wildfire of 2010. Epidemiology. 2014; 25(3):359–364. [PubMed: 24598414]

Shaposhnikov D, Revich B, Bellander T, et al. Long-term impact of Moscow heat wave and wildfires on mortality. Epidemiology. 2015; 26(2):e21–e22. [PubMed: 25643114]

Sillman J, Kharin VV, Zhang X, Zwiers FW, Bronaugh D. Climate extremes indices in the CMIP5 multimodel ensemble: part 1. Model evaluation in the present climate. J Geophys Res Atmos. 2013; 118:1716.

Stone B, Vargo J, Liu P, et al. Avoided heat-related mortality through climate adaptation strategies in three US cities. PLoS ONE. 2014; 9(6):e100852. [PubMed: 24964213]

Thomson AM, Calvin KV, Smith SJ, et al. RCP4.5: a pathway for stabilization of radiative forcing by 2100. Clim Chang. 2011; 109:77–94.

Toulemon L, Barbieri M. The mortality impact of the August 2003 heat wave in France: Investigating the 'harvesting' effect and other long-term consequences. Popul Stud. 2008; 62(1):39–53.

van Vuuren DP, Edmonds J, Kainuma M, et al. The representative concentration pathways: an overview. Clim Chang. 2011; 109:5–31.

Vandentorren S, Suzan F, Medina S, et al. Mortality in 13 French cities during the August 2003 heat wave. Am J Public Health. 2004; 94(9):1518–1520. [PubMed: 15333306]

Wu J, Zhou Y, Gao Y, et al. Estimation and uncertainty analysis of impacts of future heat waves on mortality in the eastern United States. Environ Health Perspect. 2014; 122:10–16. [PubMed: 24192064]

Zhao L, Lee X, Smith RB, Oleson K. Strong contributions of local background climate to urban heat islands. Nature. 2014; 511:216–219. [PubMed: 25008529]

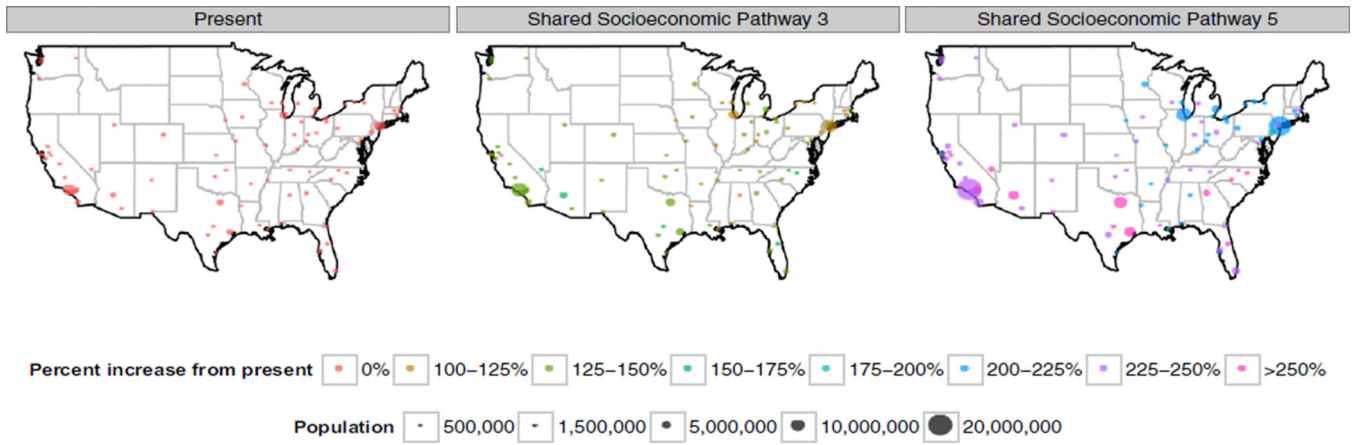**Fig. 1.**
Study communities. Each dot shows one of 82 study communities. *Dot size* indicates population at present or for a population scenario. *Dot color* shows, for projected populations, percent population increase compared to present
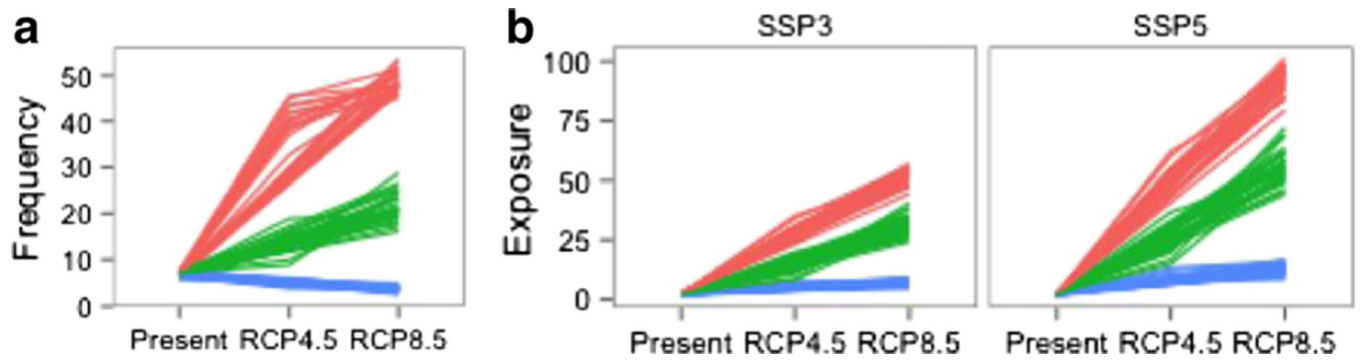
Fig. 2.

Projected trends in high-mortality heatwaves ([a] frequency and [b] exposure) under different adaptation and climate scenarios. Each line connects three projections for an ensemble member, with points for projections for present-day (*left*) and for two scenarios of greenhouse gas forcing (RCP4.5 [middle] and RCP8.5 [*right*]). "Frequency" (**a**) indicates total number of high-mortality heatwaves projected for all 82 study communities. "Exposure" (**b**) indicates total expected exposure across all 82 communities in millions of person-days per year. Color corresponds to the adaptation assumption: none (*red*), lagged (*green*), or on-pace (*blue*). All projections are based on the bagging health-based model, and all projections for (**a**) are based on the SSP3 population projection

Table 1

Heatwave characteristics considered in health-based models. Listed are all heatwave characteristics considered as potential predictive variables in the health-based models built to classify heatwaves as high-mortality or moderate, as well as the component(s) of future scenarios that influence each variable

Variable	Variable influenced by scenario			Variable included in model			
	Climate	Population	Adaptation	Simple	Tree	Bagging	Boosting
Absolute intensity							
Average of daily T_{mean} during the heatwave	X					X	
Highest daily T_{mean} during the heatwave	X					X	
Lowest daily T_{mean} during the heatwave	X						
Timing							
Day of year the heatwave started	X					X	
Month the heatwave started	X				X	X	X
Whether the heatwave was the first of the year	X					X	
Length							
Length in days	X					X	
Community climate							
Community's average annual T_{mean}	X		X			X	X
Community's average warm-season T_{mean}	X		X			X	
Relative intensity							
Quantile of average daily T_{mean}	X		X			X	
Quantile of highest daily T_{mean}	X		X	X	X	X	X
Quantile of lowest daily T_{mean}	X		X			X	
Combined length and absolute intensity							
Number of days with $T_{mean} > 80$ °F	X					X	
Number of days with $T_{mean} > 85$ °F	X					X	
Number of days with $T_{mean} > 90$ °F	X					X	
Number of days with $T_{mean} > 95$ °F	X					X	X

Variable	Variable influenced by scenario			Variable included in model		
	Climate	Population	Adaptation	Simple	Tree	Bagging	Boosting
Combined length and relative intensity						
Number of days with $T_{mean} > 99$th percentile	X		X			X
Number of days with $T_{mean} > 99.5$th percentile	X		X			X
Community population						
Community's population		X				X
Community's population density		X				

Table 2

Number of and exposure to high-mortality heatwaves projected under scenarios of climate change (RCP4.5, RCP8.5), population change (SSP3, SSP5), adaptation to climate change (none, lagged, on-pace), and health-based model. Each estimate gives the mean across ensemble members of that climate scenario (14 ensemble members for RCP4.5; 29 for Present and RCP8.5). Numbers of high-mortality heatwaves are totaled across all 82 study communities. Exposures are yearly averages, in millions of person-days per year, totaled across all 82 communities. Ranges across ensemble members are given in parentheses, and the percent of all heatwaves or heatwave exposure projected to be from high-mortality heatwaves is given after the comma in each table cell

Model	Present	Climate scenario: RCP4.5		Climate scenario: RCP8.5	
		Population scenario: SSP3	Population scenario: SSP5	Population scenario: SSP3	Population scenario: SSP5
Number of high-mortality heatwaves over a 20-year period					
No adaptation					
Classification tree	6 (5, 7), 0.22 %	43 (35, 49), 0.40 %	43 (35, 49), 0.40 %	50 (47, 55), 0.39 %	50 (47, 55), 0.39 %
Bagging	6 (5, 6), 0.19 %	41 (33, 46), 0.37 %	41 (34, 46), 0.38 %	49 (45, 53), 0.38 %	49 (46, 54), 0.38 %
Boosting	5 (4, 5), 0.17 %	36 (29, 40), 0.33 %	36 (29, 40), 0.33 %	43 (40, 47), 0.33 %	43 (40, 47), 0.33 %
Simple	6 (5, 6), 0.19 %	48 (40, 55), 0.45 %	48 (40, 55), 0.45 %	76 (70, 85), 0.59 %	76 (70, 85), 0.59 %
Lagged adaptation					
Classification tree	6 (5, 7), 0.22 %	15 (11, 21), 0.14 %	15 (11, 21), 0.14 %	24 (17, 30), 0.18 %	24 (17, 30), 0.18 %
Bagging	6 (5, 6), 0.19 %	13 (9, 19), 0.12 %	14 (9, 20), 0.13 %	22 (16, 29), 0.17 %	22 (17, 29), 0.17 %
Boosting	5 (4, 5), 0.17 %	12 (8, 16), 0.11 %	12 (8, 16), 0.11 %	19 (14, 25), 0.15 %	19 (14, 25), 0.15 %
Simple	6 (5, 6), 0.19 %	15 (11, 20), 0.14 %	15 (11, 20), 0.14 %	28 (22, 36), 0.22 %	28 (22, 36), 0.22 %
On-pace adaptation					
Classification tree	6 (5, 7), 0.22 %	6 (4, 7), 0.05 %	6 (4, 7), 0.05 %	4 (3, 6), 0.03 %	4 (3, 6), 0.03 %
Bagging	6 (5, 6), 0.19 %	5 (4, 6), 0.04 %	5 (4, 6), 0.05 %	4 (3, 5), 0.03 %	4 (3, 5), 0.03 %
Boosting	5 (4, 5), 0.17 %	4 (3, 5), 0.04 %	4 (3, 5), 0.04 %	3 (2, 4), 0.03 %	3 (2, 4), 0.03 %
Simple	6 (5, 6), 0.19 %	5 (5, 6), 0.05 %	5 (5, 6), 0.05 %	5 (4, 6), 0.04 %	5 (4, 6), 0.04 %
Exposure to high-mortality heatwaves, in millions of person-days per year					
No adaptation					
Classification tree	2 (2, 3), 0.36 %	30 (24, 36), 0.70 %	53 (42, 64), 0.70 %	53 (45, 58), 0.72 %	92 (79, 102), 0.72 %
Bagging	2 (2, 2), 0.32 %	29 (24, 35), 0.67 %	52 (43, 62), 0.68 %	52 (44, 57), 0.71 %	93 (79, 101), 0.71 %
Boosting	2 (1, 2), 0.28 %	25 (20, 31), 0.59 %	44 (36, 54), 0.59 %	46 (39, 50), 0.62 %	80 (68, 88), 0.62 %

Model	Present	Climate scenario: RCP4.5		Climate scenario: RCP8.5	
		Population scenario: SSP3	Population scenario: SSP5	Population scenario: SSP3	Population scenario: SSP5
Simple	2 (2, 2), 0.29 %	30 (25, 33), 0.68 %	52 (45, 58), 0.68 %	69 (65, 77), 0.89 %	122 (114, 136), 0.89 %
Lagged adaptation					
Classification tree	2 (2, 3), 0.36 %	14 (9, 21), 0.33 %	24 (16, 37), 0.33 %	33 (25, 42), 0.44 %	57 (44, 73), 0.44 %
Bagging	2 (2, 2), 0.32 %	13 (8, 20), 0.29 %	23 (15, 37), 0.30 %	31 (24, 41), 0.41 %	56 (44, 72), 0.42 %
Boosting	2 (1, 2), 0.28 %	11 (7, 17), 0.25 %	19 (12, 30), 0.25 %	26 (21, 35), 0.36 %	47 (36, 61), 0.36 %
Simple	2 (2, 2), 0.29 %	12 (10, 16), 0.29 %	22 (17, 29), 0.29 %	40 (34, 52), 0.51 %	71 (60, 91), 0.51 %
On-pace adaptation					
Classification tree	2 (2, 3), 0.36 %	6 (4, 8), 0.14 %	10 (7, 15), 0.14 %	8 (5, 10), 0.11 %	13 (9, 17), 0.11 %
Bagging	2 (2, 2), 0.32 %	5 (4, 7), 0.12 %	9 (7, 13), 0.12 %	7 (5, 9), 0.09 %	13 (9, 17), 0.09 %
Boosting	2 (1, 2), 0.28 %	4 (3, 6), 0.10 %	7 (5, 11), 0.10 %	6 (4, 7), 0.08 %	10 (7, 13), 0.08 %
Simple	2 (2, 2), 0.29 %	5 (4, 6), 0.12 %	9 (8, 10), 0.12 %	10 (8, 12), 0.13 %	18 (15, 22), 0.13 %